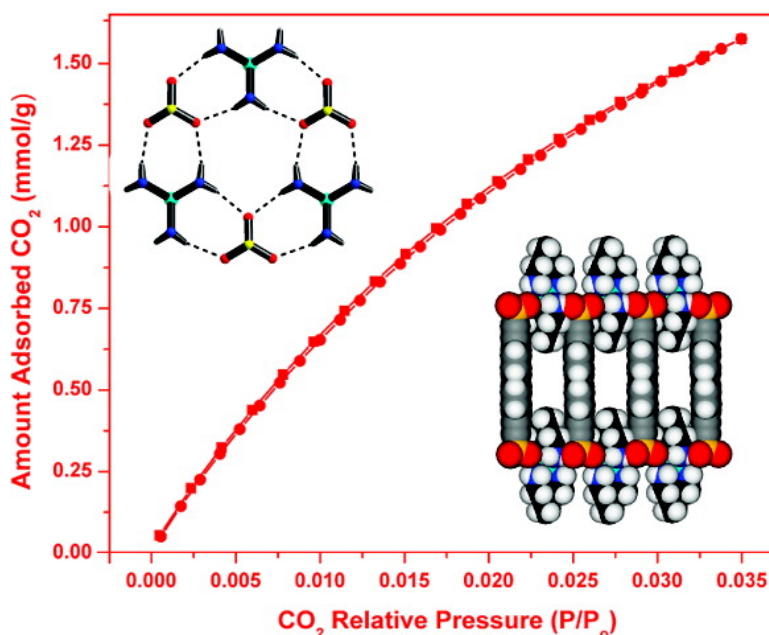


## Crystal Engineering of a Permanently Porous Network Sustained Exclusively by Charge-Assisted Hydrogen Bonds

Sean A. Dalrymple, and George K. H. Shimizu

*J. Am. Chem. Soc.*, **2007**, 129 (40), 12114-12116 • DOI: 10.1021/ja076094v • Publication Date (Web): 19 September 2007

Downloaded from <http://pubs.acs.org> on February 14, 2009



### More About This Article

Additional resources and features associated with this article are available within the HTML version:

- Supporting Information
- Links to the 10 articles that cite this article, as of the time of this article download
- Access to high resolution figures
- Links to articles and content related to this article
- Copyright permission to reproduce figures and/or text from this article

[View the Full Text HTML](#)

## Crystal Engineering of a Permanently Porous Network Sustained Exclusively by Charge-Assisted Hydrogen Bonds

Sean A. Dalrymple and George K. H. Shimizu\*

Department of Chemistry, University of Calgary, Calgary, Alberta, T2N 1N4 Canada

Received August 17, 2007; E-mail: gshimizu@ucalgary.ca

In the synthesis of network solids from molecular components, that is, crystal engineering,<sup>1</sup> two omnipresent challenges are the ability to accurately design an infinite assembly based on the structures of molecular building blocks and the ability to generate permanent pores in the material.<sup>2</sup> For solids based upon weaker interactions<sup>3</sup> (i.e., excluding covalent bonding or strong M–O bonding), the difficulties raised by these two issues are both alleviated and aggravated. Using noncovalent interactions allows reversibility during assembly, giving access to the thermodynamic product. This supramolecular “error-checking”<sup>4</sup> facilitates formation of designed products. However, formation of a porous solid requires that the network sustaining interactions are of sufficient strength to pay the energetic penalty for existence of the pores themselves. In this sense, weak interactions are clearly unfavorable.

With regards to H-bonded assemblies, guanidinium sulfonates (GS) are a family of inclusion solids based upon quasihexagonal 2-D sheets where guanidinium cations act as spacers in a layer for organosulfonate groups.<sup>5</sup> Use of disulfonates then pillars the layers in the perpendicular direction, forming interlayer channels.<sup>6</sup> Variation of organic pillars and guests has resulted in hundreds of inclusion solids that fall within only a handful of major structural motifs.<sup>6c</sup> The sheets in these structures are sustained by a hexagonal H-bonding motif that optimizes H-bonds between the 3-fold complementary guanidinium and sulfonate groups. While persistent motifs are observed, the robustness of these solids is not such that permanent porosity, as confirmed by gas sorption, has ever been reported.

Inspired by such structures, we<sup>7</sup> and others<sup>8</sup> have reported systems based on  $[\text{Co}(\text{NH}_3)_6]^{3+}$  organosulfonates. The rationale being that, as H-bond donors, the triangular faces of an octahedral hexamine complex could function analogously to two staggered guanidinium cations. Thus, with a polyvalent metal ion, increased charge assistance to the interactions and, hence, more robust solids could be expected. To date, this approach has resulted in networks which show guest inclusion<sup>7b</sup> and exchange properties,<sup>7c</sup> but as with their GS counterparts, permanent porosity has not been attainable. For these  $[\text{Co}(\text{NH}_3)_6]^{3+}$  sulfonates, the large majority of structures do not adopt an optimal “GS-like” H-bonding motif, rather the metal octahedra preferably align with their  $C_4$  axis perpendicular to the layers.<sup>7,8</sup> This owes to the fact that the  $C_3$  orientation requires a divalent cation, but unfortunately,  $[\text{M}(\text{NH}_3)_6]^{2+}$  ions are not hydrolytically stable. Beyond that, the  $\text{M}^{3+}$  system requires 50% more charge balancing pillars so that even the stoichiometry of the solid is not ideal.

Herein, we report design optimization of both the metal complex and organosulfonate pillars to enable both the idealized hexagonal H-bonding motif and, consequently, a robust and porous H-bonded network. The monosulfonate complex,  $\{[\text{Ni}(\text{tame})_2]_1(\text{PES})_2\}_\infty$  (tame = 1,1,1-tris(aminomethyl)ethane, PES = 2-phenylethynylsulfonate), **1**, was structurally characterized to reveal the ideal H-bonded layer structure. The pillared disulfonate analogue of **1**,  $\{[\text{Ni}(\text{tame})_2]_1-$

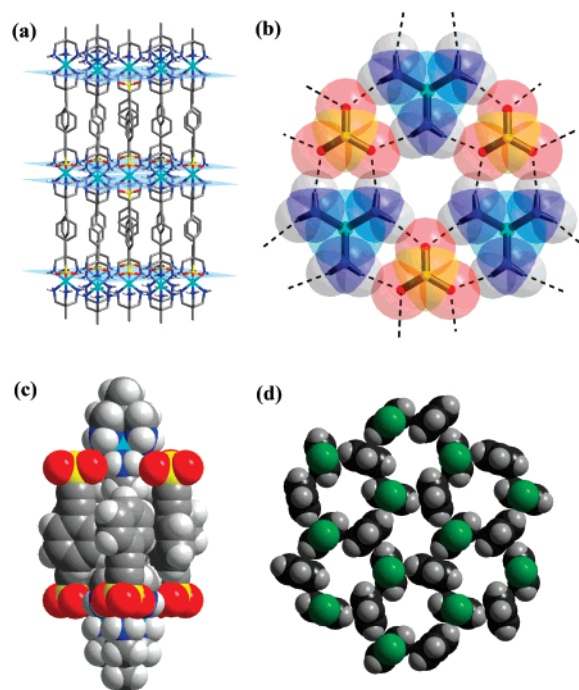


**Figure 1.** The crystal structure of **1**. (a) View of the charge-assisted H-bonded sheets (shown as blue planes) and the aromatic interlayer. (b) Overlaid space-filling diagram of the complementary H-bonds between  $\text{Ni}(\text{tame})_2^{2+}$  and PES  $\text{SO}_3$  groups. (c) Space-filling view of  $\text{Ni}(\text{tame})_2^{2+}$  units and the interdigitation of PES ligands from adjacent sheets. (d) Aryl-aryl interactions in the interlayer with aromatic groups from the same sheets marked in green. The visible voids are largely filled by the methyl groups of the tame ligands. (For a–c: Ni, cyan; N, blue; C, gray; H, white; S, yellow; O, red.)

$(\text{BSEB})_1\}_\infty$  (BSEB = 4,4'-bis(sulfoethynyl)biphenyl), **2e**, was also prepared. The unit cell of **2e**, as derived from Pawley fitting of PXRD data, indicated a similar pillared layered structure as observed in **1**. Reversible  $\text{CO}_2$  and  $\text{N}_2$  sorption isotherms confirmed **2e** displayed permanent porosity. *Compound 2e, to the best of our knowledge, is the first example of a permanently porous solid sustained exclusively by charge-assisted H-bonds. Furthermore, the structure is exactly that which was designed from the molecular precursors.*

Crystals of  $\{[\text{Ni}(\text{tame})_2]_1(\text{PES})_2\}_\infty$ , **1**, as purple trigonal plates, were grown by slowly diffusing aqueous equimolar solutions of  $\text{Ni}(\text{tame})_2\text{Cl}_2$  and NaPES together over 2 weeks. The single-crystal structure of **1**<sup>9</sup> revealed the formation of quasihexagonal H-bonded sheets which interact in the third dimension through stacking of the PES aromatic rings (Figure 1a). The sheets, which run parallel to the crystallographic  $ab$  plane, are sustained by charge-assisted H-bonds between  $\text{Ni}(\text{tame})_2^{2+}$  units and two sets of PES sulfonate groups ( $\text{N}\cdots\text{O} = 3.077\text{--}3.099 \text{ \AA}$ ). In this manner, each metal complex forms part of two parallel H-bonded sheets, the compo-

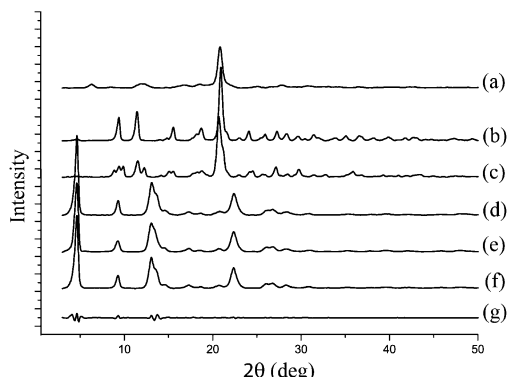


**Figure 2.** PXRD patterns for the Ni(tame)<sub>2</sub>(BSEB) phases. (a) Bulk precipitate, **2a**; (b) **2b** formed by refluxing **2a** in water; (c) **2c**, formed by dehydrating **2b**; (d) **2d**, formed by refluxing **2a** in water/benzene; (e) **2e**, formed by desolvating **2d**; (f) Pawley fitting for the indexed unit cell of **2e**; (g) difference plot between (e) and refined profiles (f).

nents of which are mutually staggered by 60° due to the octahedral metal ion's C<sub>3</sub> orientation. The spacing between the coupled sheets is 2.624 Å. As seen in Figure 1b, each tame molecule and SO<sub>3</sub><sup>−</sup> group form three pairs of H-bonds with trigonally arranged partners akin to the GS motif.<sup>10</sup> Perpendicular to the layers, PES phenyl groups interdigitate (Figure 1c) resulting in a *d*-spacing between sheets of 11.669 Å. Figure 1d shows a space-filling view of the aryl–aryl interactions within the interlayer. Each phenyl group forms one face-to-face (2.930 Å) and two edge-to-face (3.051 Å) aryl interactions solely with PES aryl rings from the adjacent sheet. The structure of **1** is a compromise between electrostatic, aryl–aryl, and H-bond interactions. The primary arrangement of components is dictated by electrostatics, above which the other interactions are balanced.

With respect to porous H-bonded solids, compared to the [Co(NH<sub>3</sub>)<sub>6</sub>]<sup>3+</sup> systems we originally reported,<sup>7</sup> **1** incorporates two major design changes. The first relates to the fact that, for a metal complex to behave analogously to two guanidinium cations, the metal ion should be divalent, but [M(NH<sub>3</sub>)<sub>6</sub>]<sup>2+</sup> ions are not hydrolytically stable. Therefore, to stabilize the 2+ state while offering trigonal pairs of N–H donors, the tripodal chelating ligand, tame, was prepared.<sup>11</sup> The second change is more subtle. Modeling studies showed that, for ideal hexagonal H-bonded assemblies between Ni(tame)<sub>2</sub><sup>2+</sup> and potentially pillaring aromatic sulfonates (e.g., biphenyldisulfonate), the protons of the methylene bridges in tame and the α-H's of the sulfonate aryl rings experienced considerable steric congestion.<sup>12</sup> The pillaring organosulfonate ligands have therefore had ethynyl spacers inserted between the SO<sub>3</sub><sup>−</sup> groups and the aromatic rings, thereby removing any deleterious α-H's. *These modifications are both necessary to enable the ideal GS-like sheet assembly in 1.* Although no porosity was observed in **1**, none was expected as a nonpillaring monosulfonate anion was employed. However, with a linear and rigid disulfonate as a pillar, the H-bonded sheets would be propped apart and porosity could be anticipated.

To construct a pillared analogue of **1**, the disulfonate BSEB anion was synthesized (see Supporting Information). Mixing aqueous solutions of Ni(tame)<sub>2</sub>Cl<sub>2</sub> and Na<sub>2</sub>BSEB resulted in an immediate precipitate, **2a**, which infers a robust network had been formed. Many efforts to obtain single crystals of **2a–2e** were unsuccessful, so powder X-ray diffraction (PXRD) studies were carried out (Figure 2). The bulk precipitate, **2a**, formulated from thermogravimetric (TGA) and elemental (EA) analyses as {[Ni(tame)<sub>2</sub>](BSEB)(H<sub>2</sub>O)}<sub>∞</sub> (Figure 2a) can be converted to a dihydrate phase, {[Ni(tame)<sub>2</sub>](BSEB)(H<sub>2</sub>O)<sub>2</sub>}<sub>∞</sub>, **2b** (Figure 2b), by refluxing in water

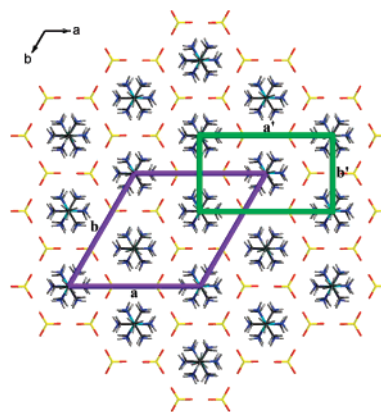


**Figure 3.** Structure of a H-bonded layer of **1**. The crystallographic *a*- and *b*-axes are shown in purple. A plausible unit cell for **2e** with parameters, *a*' = 13.86 Å and *b*' = 8.00 Å, is outlined in green.

for 12 h. Dehydration of **2b** results in a phase change, as evidenced by the shift of the low-angle 2θ peaks in the PXRD pattern, forming **2c** (Figure 2c). A CO<sub>2</sub> sorption isotherm for **2c** showed a Type I profile indicative of a microporous material with a Brunauer–Emmett–Teller (BET) surface area of 70 m<sup>2</sup>/g.<sup>13</sup> More importantly, if **2a** was refluxed in 50:50 water/benzene for 12 h, a PXRD pattern indicative of a layered solid (Figure 2d) was obtained. Refluxing in an aromatic was employed as, from analogy to **1**, the hexagonal structure places pillars at a distance appropriate to fit aryl guests. This material loses guests rapidly, but EA and TGA both showed that the sample, after equilibration under ambient conditions, could be formulated as {[Ni(tame)<sub>2</sub>](BSEB)(H<sub>2</sub>O)<sub>0.6</sub>}<sub>∞</sub>, **2d**. Desolvation of this material (3 h at 150 °C) altered neither PXRD peak positions nor intensities (Figure 2e), suggesting the formation of guest-free {[Ni(tame)<sub>2</sub>](BSEB)}<sub>∞</sub> phase, **2e**. Differential scanning calorimetry (DSC)/TGA showed that **2e** was stable to 260 °C.

To extract structural data on **2e**, the PXRD pattern was indexed.<sup>14</sup> Several potential unit cells were identified through DICVOL91 using all peaks under 25° 2θ. Pawley refinement on these unit cells (using profile fitting, fwhm, and asymmetry correction parameters) against the full powder pattern gave a monoclinic unit cell (*a*' = 13.865, *b*' = 7.794, *c*' = 19.379 Å, β' = 100.63°) based on the best fit parameters: *R*<sub>wp</sub> = 0.1066 and *R*<sub>p</sub> = 0.0730 (Figure 2f). The difference plot (Figure 2g) between calculated and experimental PXRD patterns shows an excellent fit for the refined unit cell. Key structural data can be extracted by comparing the indexed unit cell of **2e** with the crystal structure of **1** as the Ni(tame)<sub>2</sub>–sulfonate layers should be identical in the two solids. Figure 3 shows the hexagonal Ni(tame)<sub>2</sub>–sulfonate layer observed in **1** with the trace of its unit cell in purple.<sup>9</sup> A second very plausible unit cell for this sheet (in green) has parameters of *a*' = 13.86 Å and *b*' = 8.00 Å, γ' = 90°. This is in excellent accord with the refined unit cell obtained from the indexing of **2e** (*a*' = 13.865 Å, *b*' = 7.794 Å, γ = 90°) giving strong support that the ideal H-bonded array has formed. This point is corroborated by the match of the calculated and expected *c*'-axes for **2e**. With the *a*'- and *b*'-axes laying in the plane of the Ni(tame)<sub>2</sub> ions, the *c*'-axis would be orthogonal to the layers. With a hexagonal H-bonded layer and orthogonal BSEB pillars, *c*' is predicted as 19.151 Å.<sup>15</sup> The indexed *c*'-axis for **2e** is 19.379 Å. While this is a good correlation, accounting for the indexed β value of 100.63°, the interlayer spacing becomes 19.039 Å, which is an even closer fit with the predicted structure. The quality of the data did not allow Rietveld refinement. Ultimately, however, a model of the proposed structure was built on the Pawley-derived unit cell (see Supporting Information) which showed a good correlation with

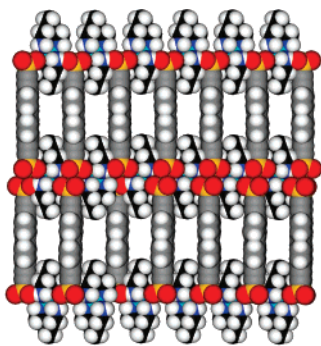


**Figure 4.** Proposed structure of **2e**, from a comparison of the unit cell of **1** and the Pawley fit PXRD of **2e**, showing layers of Ni(tame)<sub>2</sub> units (C: black) pillared by BSEB anions (C: gray) to form pores.

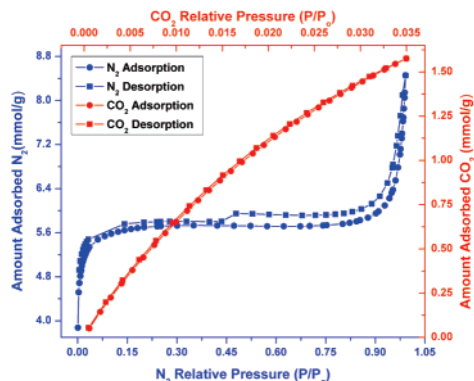


**Figure 5.** CO<sub>2</sub> (red) and N<sub>2</sub> (blue) sorption/desorption isotherms for **2e**<sup>13</sup> showing Type 1 and 2b behavior, respectively.

the observed PXRD. *On the basis of this evidence, we believe 2e has the desired and designed structure of GS-like H-bonded sheets pillared by the BSEB ligands (Figure 4).*

CO<sub>2</sub> and N<sub>2</sub> sorption isotherms were measured on **2e** and confirmed permanent porosity (Figure 5). A Type 1 isotherm was observed for CO<sub>2</sub>, giving surface areas of 326, 373, and 380 m<sup>2</sup>/g for BET, Langmuir, and Dubinin–Radushkevich (DR) models, respectively.<sup>13</sup> The isotherm does not reach saturation, and no hysteresis is seen. With N<sub>2</sub>, a Type 2b isotherm was observed,<sup>16</sup> giving surface areas of 392, 565, and 561 m<sup>2</sup>/g for BET, Langmuir, and DR models, respectively. Type 2b isotherms are typically associated with slit-shaped pores,<sup>16</sup> which is in keeping with our structure. For reference, the surface area of **2e** is greater than that of most naturally occurring zeolites.<sup>16</sup> Moreover, the pores are regular, and obvious options for increasing their size exist. Other porous solids are known where noncovalent interactions augment stronger bonds<sup>3a,17</sup> or where neutral molecules pack inefficiently.<sup>18</sup> Also, H-bonded networks capable of guest exchange are known.<sup>19</sup> To the best of our knowledge, **2e** is the only example of a permanently porous solid sustained exclusively by charge-assisted hydrogen bonds. An advantage of weak interactions is that, while **2e** is not formed by the initial self-assembly, the solid can optimize to form the ideal porous phase. A second advantage would be that, if chemistry can be done in the pores of **2e**, products could be extracted by facile disassembly (versus, say, a zeolite) followed by host regeneration. Thus, these solids offer different applications than traditional porous materials.

**Acknowledgment.** The authors thank Dr. B. Chandler for help with the indexing, Dr. J. Hill (U. of Calgary, Chem. Eng.) for access

to gas sorption analysis, the Natural Sciences and Engineering Research Council (NSERC) of Canada, the Alberta Ingenuity Fund, and the International Centre for Diffraction Data for support.

**Supporting Information Available:** Synthesis of **1**, Na<sub>2</sub>BSEB, and **2**, CIF file for **1**, and characterization (EA, TGA/DSC, IR, sorption) for all compounds. This material is available free of charge via the Internet at <http://pubs.acs.org>.

## References

- (1) (a) Desiraju, G. R. *Acc. Chem. Res.* **2002**, *35*, 565. (b) Brammer, L. *Chem. Soc. Rev.* **2004**, *33*, 476. (c) Braga, D.; Grepioni, F.; Desiraju, G. R. *Chem. Rev.* **1998**, *98*, 1375. (d) Moulton, B.; Zaworotko, M. J. *Chem. Rev.* **2001**, *101*, 1629.
- (2) (a) Kitagawa, S.; Kitaura, R.; Noro, S.-i. *Angew. Chem., Int. Ed.* **2004**, *43*, 2334. (b) Li, H.; Eddaoudi, M.; O’Keeffe, M.; Yaghi, O. M. *Nature* **1999**, *402*, 276. (c) Biradha, L.; Hongo, Y.; Fujita, M. *Angew. Chem., Int. Ed.* **2000**, *39*, 3843.
- (3) (a) Kitagawa, S.; Uemura, K. *Chem. Soc. Rev.* **2005**, *34*, 109. (b) Ripmeester, J. A.; Enright, G. D.; Ratcliffe, C. I.; Udachin, K. A.; Moudrakovski, I. L. *Chem. Commun.* **2006**, 4986. (c) Beatty, A. M. *Coord. Chem. Rev.* **2003**, *246*, 131. (d) Biradha, K.; Dennis, D.; MacKinnon, V. A.; Sharma, C. V. K.; Zaworotko, M. J. *J. Am. Chem. Soc.* **1998**, *120*, 11894. (e) Ward, M. D. *Chem. Commun.* **2005**, 5838. (f) Aakeroy, C. B.; Seddon, S. R. *Chem. Soc. Rev.* **1993**, *22*, 397. (g) Nangia, A. *Curr. Opin. Solid State Mater. Sci.* **2001**, *5*, 115.
- (4) Lehn, J. M. *Chem. Soc. Rev.* **2007**, *36*, 151.
- (5) (a) Russell, V. A.; Etter, M. C.; Ward, M. D. *J. Am. Chem. Soc.* **1994**, *116*, 1941. (b) Russell, V. A.; Ward, M. D. *J. Mater. Chem.* **1997**, *7*, 1123. (c) Martin, S. M.; Yonezawa, J.; Horner, M. J.; Macosko, C. W.; Ward, M. D. *Chem. Mater.* **2004**, *16*, 3045.
- (6) (a) Russell, V. A.; Evans, C. C.; Li, W.; Ward, M. D. *Science* **1997**, *276*, 575. (b) Holman, K. T.; Martin, S. M.; Parker, D. P.; Ward, M. D. *J. Am. Chem. Soc.* **2001**, *123*, 4421. (c) Holman, K. T.; Pivovar, A. M.; Ward, M. D. *Science* **2001**, *294*, 1907.
- (7) (a) Dalrymple, S. A.; Shimizu, G. K. H. *Chem. Commun.* **2002**, 2224. (b) Reddy, D. S.; Duncan, S.; Shimizu, G. K. H. *Angew. Chem., Int. Ed.* **2003**, *42*, 1360. (c) Dalrymple, S. A.; Shimizu, G. K. H. *Chem. Commun.* **2006**, 956. (d) Dalrymple, S. A.; Shimizu, G. K. H. *Supramol. Chem.* **2003**, *15*, 591.
- (8) (a) Bala, R.; Sharma, R. P.; Bond, A. D. J. *Mol. Struct.* **2007**, *830*, 198. (b) Wang, X. Y.; Justice, R.; Sevov, S. C. *Inorg. Chem.* **2007**, *46*, 4626.
- (9) Single-crystal X-ray data for **1**: {[Ni(tame)<sub>2</sub>]<sub>1</sub>(PES)<sub>2</sub>}<sub>∞</sub>, C<sub>26</sub>H<sub>40</sub>N<sub>6</sub>Ni<sub>1</sub>O<sub>6</sub>S<sub>2</sub>, *M* = 655.47, trigonal, space group *P*3 (No. 147), *a* = 13.862(5) Å, *c* = 13.784(5) Å, *V* = 2293.8(14) Å<sup>3</sup>, *Z* = 3, *D<sub>c</sub>* = 1.424 mg m<sup>-3</sup>, μ(*Mo Kα*) = 0.820 mm<sup>-1</sup>, crystal size 0.22 × 0.20 × 0.15 mm. A total of 6703 reflections (3.39° < θ < 27.48°) were processed, of which 3488 were unique and significant with *I*<sub>net</sub> > 2σ(*I*<sub>net</sub>). Final residuals were *R* = 0.0398 and *R<sub>w</sub>* = 0.0989 (GoF = 1.045) for 190 parameters.
- (10) Through graph set notation theory, each pair of H-bonding interactions can be described as *R*<sub>2</sub><sup>2</sup>(8) dimers which, when aligned through crystal symmetry, form *R*<sub>6</sub><sup>3</sup>(12) rings between molecular components. Etter, M. C.; MacDonald, J. C.; Bernstein, J. *Acta Crystallogr.* **1990**, *B46*, 256.
- (11) Geue, J. G.; Searle, G. H. *Aust. J. Chem.* **1983**, *36*, 927.
- (12) Close packing interactions between the desired arrangement of molecular building blocks with constrained hexagonal hydrogen bonding environments (N–H···O = 1.5–2.2 Å) were examined with *Discovery Studio ViewerPro 5.0*; Accelrys Inc.: San Diego, CA, 2004.
- (13) CO<sub>2</sub> (273 K) and N<sub>2</sub> (77 K) surface area measurements were made on a Micromeritics Tristar 3000 Analyzer after outgassing, for 4 h at 175 °C.
- (14) Indexing and refinement was performed with the *Reflex module of Materials Studio Modeling 4.0*; Accelrys Inc.: San Diego, CA, 2005.
- (15) The predicted interlayer Ni(tame)<sub>2</sub><sup>2+</sup> spacing of 19.145 Å was calculated from the length of the BSEB ligand (16.597 Å) plus the distance between Ni<sup>2+</sup> and the mean H-bond donor plane of the coordinated tame ligands (2 × 1.273 Å) as taken from crystallographic data of **1**.
- (16) Rouquerol, F.; Rouquerol, J.; Sing, K. *Adsorption by Powders and Porous Solids*; Academic Press: London, 1999.
- (17) (a) Soldatov, D. V.; Moudrakovski, I.; Ripmeester, J. A. *Angew. Chem., Int. Ed.* **2004**, *43*, 6308. (b) Dewal, M. B.; Lufaso, M. W.; Hughes, A. D.; Samuel, S. A.; Pellechia, P.; Shimizu, L. S. *Chem. Mater.* **2006**, *18*, 4855.
- (18) (a) Dianin, A. P. *J. Russ. Phys. Chem. Soc.* **1914**, *31*, 1310. (b) Dalgarno, S. J.; Thallapally, P. K.; Barbour, L. J.; Atwood, J. L. *Chem. Soc. Rev.* **2007**, *36*, 236. (c) Sozzani, P.; Bracco, S.; Comotti, A.; Ferretti, L.; Simonutti, R. *Angew. Chem., Int. Ed.* **2005**, *44*, 1816.
- (19) (a) Endo, K.; Sawaki, T.; Koyanagi, M.; Kobayashi, K.; Masuda, H.; Aoyama, Y. *J. Am. Chem. Soc.* **1995**, *117*, 8341. (b) Malek, N.; Maris, T.; Simard, M.; Wuest, J. D. *J. Am. Chem. Soc.* **2005**, *127*, 5910. (c) Kepert, C. J.; Hesek, D.; Beer, P. D.; Rosseinsky, M. J. *Angew. Chem., Int. Ed.* **1998**, *37*, 3158.

JA076094V